

# Confinement and $\mathbb{Z}_3$ symmetry in three-flavor QCD

Hiroaki Kouno,<sup>1,\*</sup> Takahiro Makiyama,<sup>1,†</sup>

Takahiro Sasaki,<sup>2,‡</sup> Yuji Sakai,<sup>3,§</sup> and Masanobu Yahiro<sup>2,¶</sup>

<sup>1</sup>*Department of Physics, Saga University, Saga 840-8502, Japan*

<sup>2</sup>*Department of Physics, Graduate School of Sciences,  
Kyushu University, Fukuoka 812-8581, Japan*

<sup>3</sup>*Theoretical Research Division, Nishina Center, RIKEN, Saitama 351-0198, Japan*

(Dated: September 29, 2018)

## Abstract

We investigate the confinement mechanism in three-flavor QCD with imaginary isospin chemical potentials  $(\mu_u, \mu_d, \mu_s) = (i\theta T, -i\theta T, 0)$ , using the Polyakov-loop extended Nambu–Jona-Lasinio (PNJL) model, where  $T$  is temperature. As for three degenerate flavors, the system has  $\mathbb{Z}_3$  symmetry at  $\theta = 2\pi/3$  and hence the Polyakov loop  $\Phi$  vanishes there for small  $T$ . As for 2+1 flavors, the symmetry is not preserved for any  $\theta$ , but  $\Phi$  becomes zero at  $\theta = \theta_{\text{conf}} < 2\pi/3$  for small  $T$ . The confinement phase defined by  $\Phi = 0$  is realized, even if the system does not have  $\mathbb{Z}_3$  symmetry exactly. In the  $\theta$ - $T$  plane, there is a critical endpoint of deconfinement transition. The deconfinement crossover at zero chemical potential is a remnant of the first-order deconfinement transition at  $\theta = \theta_{\text{conf}}$ . The relation between the non-diagonal element  $\chi_{us}$  of quark number susceptibilities and the deconfinement transition is studied. The present results can be checked by lattice QCD simulations directly, since the simulations are free from the sign problem for any  $\theta$ .

PACS numbers: 11.30.Rd, 12.40.-y

---

\*kounoh@cc.saga-u.ac.jp

†12634019@edu.cc.saga-u.ac.jp

‡sasaki@phys.kyushu-u.ac.jp

§ysakai@riken.jp

¶yahiro@phys.kyushu-u.ac.jp

## I. INTRODUCTION

Lattice QCD (LQCD) simulations indicate that QCD is in the confinement and chiral symmetry breaking phase at low temperature ( $T$ ) and in the deconfinement and chiral symmetry restoration phase at high  $T$ . Understanding of the confinement mechanism is, nevertheless, not adequate, although the chiral restoration is relatively well understood. The reason mainly comes from the fact that there is no exact symmetry for the deconfinement transition and hence the order parameter is unknown. In the limit of infinite current quark mass, the Polyakov-loop [1] is an exact order parameter for the deconfinement transition, since  $\mathbb{Z}_{N_c}$  symmetry is exact there, where  $N_c$  is the number of colors. The chiral condensate is, meanwhile, an exact order parameter for the chiral restoration in the limit of zero current quark mass. In the real world where  $u$  and  $d$  quarks have small current masses  $m_l \equiv m_u = m_d$ , the chiral condensate is considered to be a good order parameter for the chiral restoration, but there is no guarantee that the Polyakov-loop  $\Phi$  is a good order parameter for the deconfinement transition.

In order to answer this problem, we constructed a gauge theory invariant under the  $\mathbb{Z}_{N_c}$  transformation, that is, a gauge theory with  $N_f$  degenerate flavor fermions having flavor-dependent fermion boundary conditions [2, 3]. This  $\mathbb{Z}_{N_c}$ -symmetric gauge theory is constructed as follow. Let us start with  $N_c$ -color QCD. The partition function  $Z$  in Euclidean spacetime is

$$Z = \int Dq D\bar{q} DA \exp[-S_0] \quad (1)$$

with the action

$$S_0 = \int d^4x \left[ \sum_f \bar{q}_f (\gamma_\nu D_\nu + m_f) q_f + \frac{1}{4g^2} F_{\mu\nu}^a{}^2 \right], \quad (2)$$

where  $q_f$  is the quark field with flavor  $f$  and current quark mass  $m_f$ ,  $D_\nu = \partial_\nu - iA_\nu$  is the covariant derivative with the gauge field  $A_\nu$ ,  $g$  is the gauge coupling and  $F_{\mu\nu} = \partial_\mu A_\nu - \partial_\nu A_\mu - i[A_\mu, A_\nu] = F_{\mu\nu}^a T^a$  for the  $SU(N_c)$  generators  $T^a$ . The temporal boundary conditions for quarks are

$$q_f(x, \beta = 1/T) = -q_f(x, 0). \quad (3)$$

The boundary conditions are changed into

$$q_f(x, \beta) = -\exp(i2\pi k/N_c) q_f(x, 0) \quad (4)$$

by the  $\mathbb{Z}_{N_c}$  transformation [1, 4–7]

$$\begin{aligned} q &\rightarrow Uq, \\ A_\nu &\rightarrow UA_\nu U^{-1} - i(\partial_\nu U)U^{-1}, \end{aligned} \quad (5)$$

where  $U(x, \tau)$  are elements of  $SU(N_c)$  with the property  $U(x, \beta) = \exp(-i2\pi k/N_c)U(x, 0)$  for integer  $k$ , while the action  $S_0$  keeps the original form (2) since  $\mathbb{Z}_{N_c}$  symmetry is the center symmetry of the gauge symmetry [6].  $\mathbb{Z}_{N_c}$  symmetry thus breaks down through the fermion boundary condition in QCD.

Now we consider the  $SU(N)$  gauge theory with  $N$  degenerate flavor quarks, i.e.  $N \equiv N_f = N_c$ , and assume the following flavor dependent twist boundary conditions (TBC):

$$\begin{aligned} q_f(x, \beta) &= -\exp(-i\theta_f)q_f(x, 0) \\ &\equiv -\exp[-i(\theta_1 + 2\pi(f-1)/N)]q_f(x, 0) \end{aligned} \quad (6)$$

for flavors  $f$  labeled by integers from 1 to  $N$ ; here  $\theta_1$  is an arbitrary real number in a range of  $0 \leq \theta_1 < 2\pi$ . The action  $S_0$  with the TBC is invariant under the  $\mathbb{Z}_{N_c}$  transformation. In fact, the  $\mathbb{Z}_{N_c}$  transformation changes  $f$  into  $f - k$ , but  $f - k$  can be relabeled by  $f$  since  $S_0$  is invariant under the relabeling. This is the gauge theory proposed in our previous works [2, 3] and is referred to as the  $\mathbb{Z}_{N_c}$ -symmetric gauge theory in this paper.

When the fermion field  $q_f$  is replaced by

$$q_f \rightarrow \exp(-i\theta_f T\tau)q_f \quad (7)$$

with Euclidean time  $\tau$ , the action  $S_0$  is changed into [7]

$$S(\theta_f) = \int d^4x \left[ \sum_f \bar{q}_f (\gamma_\nu D_\nu - \mu_f \gamma_4 + m_f) q_f + \frac{1}{4g^2} F_{\mu\nu}^2 \right] \quad (8)$$

with the imaginary quark number chemical potential  $\mu_f = iT\theta_f$ , while the TBC is transformed back to the standard one (3). The action  $S_0$  with the TBC is thus equivalent to the action  $S(\theta_f)$  with the standard one (3).

In the limit of  $T = 0$ , the  $\mathbb{Z}_{N_c}$ -symmetric gauge theory is identical with QCD with the standard boundary condition (3). Noting that  $\Phi = 0$  at  $T = 0$ , one can predict that in the  $\mathbb{Z}_{N_c}$ -symmetric gauge theory  $\mathbb{Z}_{N_c}$  symmetry is preserved up to some temperature  $T_c$  and spontaneously broken above  $T_c$ . In fact, this behavior is confirmed in Refs. [2, 3] by imposing the TBC on the Polyakov-loop extended Nambu-Jona-Lasinio (PNJL) model [8–37] that has the same global symmetries as QCD at imaginary chemical potentials. In the  $\mathbb{Z}_{N_c}$ -symmetric gauge theory, the quarkyonic phase with  $\Phi = 0$  and finite quark-number density appear at small  $T$  and large real quark-number chemical potential  $\mu$  [3].  $\mathbb{Z}_{N_c}$  symmetry is thus essential for emergence of the quarkyonic phase.

In real QCD, however, s-quark has a current quark mass  $m_s$  heavier than  $m_l$ , where  $m_l$  is a current quark mass of light quarks. This means that real QCD does not become  $\mathbb{Z}_3$ -symmetric even if the TBC is imposed. However, the TBC or its small extension may be important to understand the confinement mechanism, since real QCD with 2+1 flavors is not far from QCD with three degenerate flavors. As an extension of the TBC, one can consider the  $\theta$ -variant TBC

$$(\theta_u, \theta_d, \theta_s) = (\theta, -\theta, 0), \quad (9)$$

where  $\theta$  varies from 0 to  $\pi$ ; this boundary condition is illustrated in Fig. 1. The system with the  $\theta$ -variant TBC is equivalent to the system with imaginary isospin chemical potential

$$(\mu_u, \mu_d, \mu_s) = (i\theta T, -i\theta T, 0), \quad (10)$$

where  $\mu_1 \equiv \mu_u - \mu_d = 2i\theta T$  means the imaginary isospin chemical potential. The  $\theta$ -variant TBC agrees with the standard boundary condition (3) when  $\theta = 0$  and the TBC (6) when  $\theta = 2\pi/3$ . For the case of small  $T$ , as shown later in Sec. III,  $\Phi$  keeps a real number for any  $\theta$  and varies from a positive value to a negative one as  $\theta$  increases from 0, since charge-conjugation ( $\mathcal{C}$ ) symmetry is not spontaneously broken there. This means that  $\Phi$  becomes zero at some value  $\theta_{\text{conf}}$  of  $\theta$ . Hence the static-quark free energy,  $-T \ln[\Phi]$ , diverges there. Thus the confinement appears, even if the system does not have  $\mathbb{Z}_{N_c}$  symmetry exactly. This fact means that one can consider the confinement by using  $\Phi$  and regard it as an order parameter of the confinement/deconfinement transition, even if  $\mathbb{Z}_{N_c}$  symmetry is not preserved exactly. Thus 2+1 flavor QCD with imaginary isospin-chemical potentials (10) is an important system to be analyzed.

As for zero and real  $\mu$ , meanwhile, an important question is what is a good indicator of QCD phase transition in heavy-ion collisions. About 10 years ago, it was proposed that correlations and fluctuations (or susceptibilities) of conserved charges may be good signals [38–43]. If there exists a critical endpoint (CEP) of chiral transition [44, 45], the baryon number susceptibility may be a good signal, since it diverges at the CEP [38, 41, 42]. More recently it was suggested that third moments of conserved charges can serve as probes of the CEP [46]. Furthermore, it was proposed in Ref. [43] with the two-phase description of quark-hadron phase transition that the non-diagonal element  $\chi_{us}$  of quark number susceptibilities may be a good indicator of the confinement/deconfinement transition, since it vanishes in the deconfinement phase where interactions are weak but becomes finite in the hadron phase where different species of quarks are confined. The non-diagonal element was recently analyzed by LQCD simulations [47, 48] and the PNJL model [49, 50].

In this paper, we analyze QCD at imaginary isospin-chemical potentials (10) for both cases of three degenerate flavors and 2+1 flavors, using the PNJL model. As for three degenerate flavors, QCD with imaginary isospin-chemical potentials (10) becomes  $\mathbb{Z}_3$ -symmetric at  $\theta = 2\pi/3$  and hence  $\bar{\Phi}$  becomes zero there. As for 2+1 flavor quarks,  $\bar{\Phi}$  vanishes at  $\theta = \theta_{\text{conf}} < 2\pi/3$  and  $\theta_{\text{conf}}$  is a function of  $T$ . In the  $\theta$ - $T$  plane, there is a line of  $\bar{\Phi} = 0$  for both three degenerate flavors and 2+1 flavors. On the line, the thermodynamic potential  $\Omega$  has the same property between the two cases. For real QCD with 2+1 flavors, it is well known that the deconfinement transition is crossover at zero  $\theta$  [51]. The deconfinement crossover is a remnant of the first-order deconfinement transition at  $\theta = \theta_{\text{conf}}$ . This  $\theta$  dependence indicates that there exists a CEP of deconfinement transition in the  $\theta$ - $T$  plane.

We also investigate the interplay between the deconfinement transition and the non-diagonal element  $\chi_{us}$  of quark number susceptibilities at zero and finite  $\theta$ . The pseudocritical temperature of the deconfinement transition is usually defined by the peak position of the Polyakov-loop susceptibility. The absolute value  $|d\chi_{us}/dT|$  has a peak at the pseudocritical temperature, whereas  $\chi_{us}$  does not. This behavior is more conspicuous at the CEP than at zero  $\theta$ . In the  $\theta$ - $T$  plane, hence, a transition line defined by the peak position of  $|d\chi_{us}/dT|$  almost coincides with a transition line by the peak position of the Polyakov-loop susceptibility.

This paper is organized as follows. In §2, the three-flavor PNJL model is recapitulated and  $\theta$  dependence of  $\bar{\Phi}$  is analyzed with the PNJL model. In §3, numerical results are shown. Section 4 is devoted to a summary.

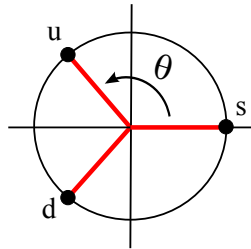


Fig. 1: The  $\theta$ -variant TBC: Location of  $e^{i\theta_f}$  ( $f = u, d, s$ ) on a unit circle in the complex plane.

## II. PNJL MODEL

The PNJL model [8–11, 13–29, 31–37] is designed to describe the confinement mechanism as well as the chiral symmetry breaking. In the imaginary  $\mu$  region, the model can reproduce LQCD data [52–62], since the model describes the Roberge-Weiss (RW) periodicity [6, 7, 18, 22, 32, 36]. The model is also successful for the imaginary isospin chemical potential region [24, 57, 58]. We recapitulate the model.

The three-flavor PNJL Lagrangian is defined in Euclidian spacetime as

$$\begin{aligned} \mathcal{L} = & \bar{q}(\gamma_\nu D_\nu + \hat{m} - \hat{\mu}\gamma_4)q - G_S \sum_{a=0}^8 [(\bar{q}\lambda_a q)^2 + (\bar{q}i\gamma_5\lambda_a q)^2] \\ & + G_D \left[ \det_{ij} \bar{q}_i(1 + \gamma_5)q_j + \text{h.c.} \right] + \mathcal{U}(\Phi[A], \Phi^*[A], T), \end{aligned} \quad (11)$$

where  $D_\nu = \partial_\nu - i\delta_{\nu 4}A_4$ ,  $\lambda_a$  is the Gell-Mann matrices,  $\hat{m} = \text{diag}(m_u, m_d, m_s)$  denotes the mass matrix and  $\hat{\mu} = \text{diag}(\mu_u, \mu_d, \mu_s)$  stands for the chemical potential matrix.  $G_S$  and  $G_D$  are coupling constants of the scalar-type four-quark and the Kobayashi-Maskawa-'t Hooft (KMT) interaction [63, 64], respectively. The KMT interaction breaks  $U_A(1)$  symmetry explicitly. The Polyakov-loop  $\Phi$  and its conjugate  $\Phi^*$  [1, 65] are defined by

$$\Phi = \frac{1}{3}\text{tr}_c(L), \quad \Phi^* = \frac{1}{3}\text{tr}_c(\bar{L}), \quad (12)$$

with  $L = \exp(iA_4/T)$  and its hermitian conjugate  $\bar{L}$ . In the PNJL model, they are calculated with the Polyakov gauge. We take the Polyakov potential of Ref. [13]:

$$\begin{aligned} \mathcal{U} = T^4 \left[ -\frac{a(T)}{2}\Phi^*\Phi \right. \\ \left. + b(T)\ln(1 - 6\Phi\Phi^* + 4(\Phi^3 + \Phi^{*3}) - 3(\Phi\Phi^*)^2) \right], \end{aligned} \quad (13)$$

$$a(T) = a_0 + a_1\left(\frac{T_0}{T}\right) + a_2\left(\frac{T_0}{T}\right)^2, \quad b(T) = b_3\left(\frac{T_0}{T}\right)^3. \quad (14)$$

Parameters of  $\mathcal{U}$  are fitted to LQCD data at finite  $T$  in the pure gauge limit. The parameters except  $T_0$  are summarized in Table I. The Polyakov potential yields the first-order deconfinement phase transition at  $T = T_0$  in the pure gauge theory [66, 67]. The original value of  $T_0$  is 270 MeV determined from the pure gauge LQCD data, but the PNJL model with this value yields a larger value of the pseudocritical temperature  $T_c$  at zero chemical potential than  $T_c \approx 160$  MeV predicted by full LQCD [68–71]. We then rescale  $T_0$  to 195 MeV so as to reproduce  $T_c \sim 160$  MeV [33].

$a_0$	$a_1$	$a_2$	$b_3$
3.51	-2.47	15.2	-1.75

TABLE I: Summary of the parameter set in the Polyakov-potential sector determined in Ref. [13]. All parameters are dimensionless.

The thermodynamic potential (per volume) is obtained by the mean-field approximation as [26]

$$\Omega = -2 \sum_{f=u,d,s} \int \frac{d^3\mathbf{p}}{(2\pi)^3} \left[ 3E_f + \frac{1}{\beta} (\ln \mathcal{F}_f + \ln \mathcal{F}_{\bar{f}}) \right. \\ \left. + U_M(\sigma_f) + \mathcal{U}(\Phi, T), \right. \quad (15)$$

where

$$\mathcal{F}_f = 1 + 3\Phi e^{-\beta E_f^-} + 3\Phi^* e^{-2\beta E_f^-} + e^{-3\beta E_f^-}, \quad (16)$$

$$\mathcal{F}_{\bar{f}} = 1 + 3\Phi^* e^{-\beta E_f^+} + 3\Phi e^{-2\beta E_f^+} + e^{-3\beta E_f^+} \quad (17)$$

with  $\sigma_f = \langle \bar{q}_f q_f \rangle$ ,  $E_f^\pm = E_f \pm \mu_f$  and  $E_f = \sqrt{\mathbf{p}^2 + M_f^2}$ . The term  $\mathcal{F}_f$  ( $\mathcal{F}_{\bar{f}}$ ) comes from a quark (antiquark) loop. For imaginary chemical potential,  $\Phi^*$  is the complex conjugate to  $\Phi$ , since  $\Omega$  is real. For imaginary isospin chemical potential,  $\Omega$  is invariant under the  $\mathcal{C}$  transformation  $\Phi \leftrightarrow \Phi^*$ , because

$$\Omega(\theta) \xrightarrow{\mathcal{C}} \Omega(-\theta) \xrightarrow{u \leftrightarrow d} \Omega(\theta), \quad (18)$$

where the second transformation is the relabeling of u and d. The three-dimensional cutoff is taken for the momentum integration in the vacuum term [26]. The dynamical quark masses  $M_f$  and the mesonic potential  $U_M$  are defined by

$$M_f = m_f - 4G_S \sigma_f + 2G_D \sigma_{f'} \sigma_{f''}, \quad (19)$$

$$U_M = \sum_{f=u,d,s} 2G_S \sigma_f^2 - 4G_D \sigma_u \sigma_d \sigma_s, \quad (20)$$

where  $f \neq f'$ ,  $f \neq f''$  and  $f' \neq f''$ .

The NJL sector of the PNJL model has six parameters,  $(G_S, G_D, m_u, m_d, m_s, \Lambda)$ . A typical set of the parameters is obtained in Ref. [72]; for example,  $m_l = m_u = m_d = 5.5$  MeV and  $m_s = 140.7$  MeV. The parameter set is fitted to empirical values of  $\eta'$ - and  $\pi$ -meson masses and  $\pi$ -meson decay constant at vacuum. We refer to this parameter set as “set R” (realistic parameter

set). For theoretical interest, furthermore, we vary the strange quark mass only as  $m_s = 5.5$  and 600 MeV. We refer to the parameter set with  $m_s = 5.5$  MeV as “set S” (symmetric parameter set) and that with  $m_s = 600$  MeV as “set H” (heavy strange quark parameter set). These parameter sets are summarized in Table II.

Set	$m_l(\text{MeV})$	$m_s(\text{MeV})$	$\Lambda(\text{MeV})$	$G_S\Lambda^2$	$G_D\Lambda^5$
R	5.5	140.7	602.3	1.835	12.36
S	5.5	5.5	602.3	1.835	12.36
H	5.5	600.0	602.3	1.835	12.36

TABLE II: Summary of the parameter sets in the NJL sector.

The resultant thermodynamic potential  $\Omega$  is a function of  $\sigma_u, \sigma_d, \sigma_s, \Phi$  and  $\Phi^*$ . Values of the mean fields are determined from the location of the global minimum of  $\Omega$  in the variable space. Since  $\sigma_u = \sigma_d$  is preserved except for the RW phase in which  $\mathcal{C}$  symmetry is spontaneously broken [22], we use  $\sigma \equiv (\sigma_u + \sigma_d + \sigma_s)/3$  and  $\sigma' = \sigma_s - (\sigma_u + \sigma_d)/2 = \sigma_u - \sigma_d$  as order parameters, and adopt  $\Phi_R = (\Phi + \Phi^*)/2$  and  $\Phi_I = (\Phi - \Phi^*)/(2i)$  instead of  $\Phi$  and  $\Phi^*$ . The order parameter  $\Phi_I$  is  $\mathcal{C}$ -odd, whereas  $\sigma, \sigma'$  and  $\Phi_R$  are  $\mathcal{C}$ -even.

The susceptibilities are calculable as [17]

$$\chi_{\varphi_i\varphi_j} \equiv (C^{-1})_{\varphi_i\varphi_j} \quad (21)$$

with the curvature matrix  $C$  defined by

$$C_{\varphi_i\varphi_j} = \frac{\partial^2 \Omega(T, \mu, \varphi)}{\partial \varphi_i \partial \varphi_j}, \quad (22)$$

where  $\varphi_1 = \sigma, \varphi_2 = \sigma', \varphi_3 = \Phi_R, \varphi_4 = \Phi_I$ . When it is not confusing, we denote the set  $\{\mu_u, \mu_d, \mu_s\}$  by  $\mu$  and the set  $\{\sigma, \sigma', \Phi_R, \Phi_I\}$  by  $\varphi$ . The Polyakov-loop susceptibilities,  $\chi_{\Phi_R\Phi_R}$  and  $\chi_{\Phi_I\Phi_I}$  are real for imaginary isospin chemical potential except for the RW-phase.

The susceptibilities of quark number densities are defined as

$$\chi_{ff'} = -\frac{D^2 \Omega(T, \mu, \varphi(T, \mu))}{D\mu_f D\mu_{f'}}, \quad (23)$$

where  $f, f' = u, d, s$  and the derivation  $\frac{D}{D\mu_f}$  means the partial derivation with respect to  $\mu_f$  with fixing the other external parameters  $T$  and  $\mu_{f''} (\neq \mu_f)$ . We also define the derivative of the susceptibilities with respect to  $T$  as

$$\chi_{ff',T} = -\frac{D\chi_{ff'}(T, \mu, \varphi(T, \mu))}{DT}. \quad (24)$$



Using the  $\mathbb{Z}_3$  transformation

$$\Phi \rightarrow e^{-i2\pi k/3}\Phi, \quad \Phi^* \rightarrow e^{i2\pi k/3}\Phi^* \quad (25)$$

with an arbitrary integer  $k$ , one can see that  $\Omega$  has the RW periodicity [6, 18, 22, 32, 36]:

$$\Omega(\theta_u, \theta_d, \theta_s) = \Omega(\theta_u + 2k\pi/3, \theta_d + 2k\pi/3, \theta_s + 2k\pi/3). \quad (26)$$

The RW periodicity does not mean that the system is  $\mathbb{Z}_3$ -symmetric, since the external parameters  $\theta_f$  are shifted by the  $\mathbb{Z}_3$  transformation. An exception is the three degenerate flavor system with  $\theta = 2\pi/3$ . In fact, the  $\theta_f$  are shifted by the  $\mathbb{Z}_3$  transformation, but the shifted  $\theta_f$  are transformed back to the original by the relabeling of flavors, as mentioned in Sec. I. In the confinement phase appearing at low  $T$  as a consequence of  $\mathbb{Z}_3$  symmetry, the thermodynamic potential is obtained by setting  $\Phi = 0$  in (15). The resultant thermodynamic potential includes only three-quark configurations  $e^{-3E_f/T}$ . As a result of this property, the flavor symmetry broken by the flavor-dependent TBC is recovered in the confinement phase [2, 3].

Finally we consider  $\theta$ -dependence of  $\Phi$  at low  $T$ . In (15),  $\Omega$  depends on  $\Phi$  only through the Polyakov-loop potential  $\mathcal{U}$  and the logarithmic term  $F \equiv -T \sum_f (\ln \mathcal{F}_f + \ln \mathcal{F}_{\bar{f}})$ . For small  $T$ , it is well satisfied that  $T \ll M_f$  and  $\Phi \ll 1$ . Hence  $F$  is approximated into

$$F \approx -6T\Phi N \quad (27)$$

with

$$N = \sum_f e^{-\beta E_f^-}, \quad (28)$$

where  $\Phi$  and  $N$  are real for any  $\theta$ , because  $\mathcal{C}$  symmetry is preserved. For small  $T$ , the Polyakov-loop potential  $\mathcal{U}$  has a global minimum at  $\Phi = 0$ . The logarithmic term then moves the minimum point to positive (negative)  $\Phi$ , when  $N$  is positive (negative). When  $\theta$  varies from 0 to  $2\pi/3$ ,  $N$  changes the sign from plus to minus. Hence the minimum point moves from positive  $\Phi$  to negative  $\Phi$  as  $\theta$  increases from 0 to  $2\pi/3$ . Eventually the confinement phase with  $\Phi = 0$  emerges at some value  $\theta_{\text{conf}}$  of  $\theta$ . It follows from  $N = 0$  that

$$\theta_{\text{conf}} \approx \arccos \left( -\frac{1}{2} e^{\beta(M_l - M_s)} \right), \quad (29)$$

and hence  $\theta_{\text{conf}} = 2\pi/3$  for three degenerate flavors ( $M_l = M_s$ ) and  $\pi/2$  for two flavors ( $M_s = \infty$ ). This indicates that  $\theta_{\text{conf}}$  is between  $2\pi/3$  and  $\pi/2$  for 2+1 flavors, whereas  $\theta_{\text{conf}} = 2\pi/3$  for set S. Thus the confinement emerges, even if  $\mathbb{Z}_3$  symmetry is not preserved. The thermodynamic potential (15) in the phase has only three-quark configurations  $e^{-3E_f/T}$  for both of three degenerate flavors and 2+1 flavors. The only difference between the two cases is the value of  $\theta_{\text{conf}}$ .

### III. NUMERICAL RESULTS

#### A. The case of $\mu = 0$

We first analyze the thermodynamics at  $\mu = 0$  through the PNJL calculation with set R. In panel (a) of Fig. 2,  $\sigma$  and  $\Phi$  are plotted as a function of  $T$ . As  $T$  increases,  $\sigma$  decreases smoothly, while  $\Phi$  increases continuously. Both the chiral and the deconfinement transition are thus crossover. Panel (b) corresponds to  $T$  dependence of susceptibilities  $\chi_{\sigma\sigma}$ ,  $\chi_{\Phi_R\Phi_R}$  and  $\chi_{\Phi_I\Phi_I}$ . Here the pseudocritical temperature  $T_C$  ( $T_D$ ) of the chiral (deconfinement) transition is defined by the temperature at which  $\chi_{\sigma\sigma}$  ( $\chi_{\Phi_R\Phi_R}$ ) becomes maximum; in the present calculation,  $T_C = 202$  MeV and  $T_D = 161$  MeV. Since  $\Phi = \Phi^*$ ,  $\Phi_I$  is zero. This means that  $\Phi_I$  itself is not a good order parameter of the deconfinement transition. The peak position of  $\chi_{\Phi_I\Phi_I}$  does not coincide with that of  $\chi_{\Phi_R\Phi_R}$ , but it should be noted that  $\chi_{\Phi_I\Phi_I}$  is rapidly changed at  $T = T_D$  where  $\chi_{\Phi_R\Phi_R}$  has a peak.

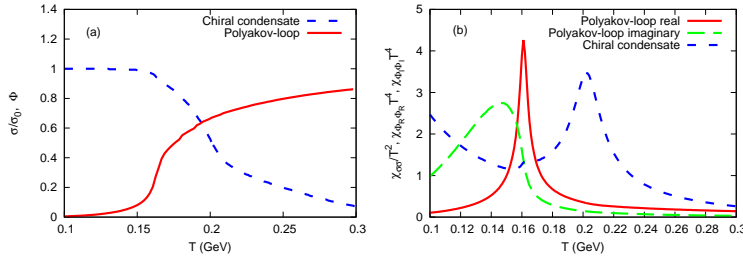


Fig. 2:  $T$  dependence of (a) the chiral condensate  $\sigma$  and the Polyakov loop  $\Phi$  and (b) their susceptibilities  $\chi_{\sigma\sigma}$ ,  $\chi_{\Phi_R\Phi_R}$  and  $\chi_{\Phi_I\Phi_I}$  at  $\mu_f = 0$ . Set R is taken in the PNJL calculation. The chiral condensate  $\sigma$  is normalized by the value  $\sigma_0$  at  $T = 0$ .  $\chi_{\Phi_R\Phi_R}$  and  $\chi_{\Phi_I\Phi_I}$  are multiplied by 10 and 100, respectively.

## B. The case of $\theta = 2\pi/3$

Next we analyze the thermodynamics at  $\theta = 2\pi/3$  through the PNJL model with set R and set S. First we consider set R. In Fig. 3(a),  $\sigma$  and  $|\Phi|$  are plotted as a function of  $T$ . The Polyakov loop  $\Phi$  is real at small  $T$  where  $\mathcal{C}$  symmetry is preserved, but becomes complex at high  $T$  where the  $\mathcal{C}$  symmetry is spontaneously broken. The high  $T$  region is called the RW phase; further discussion will be made in subsection III C for the RW phase. As  $T$  increases,  $\Phi$  has a discontinuity at  $T = T_D = 188$  MeV, whereas  $\sigma$  decreases slowly. This indicates that the deconfinement transition is the first order. Thus the imaginary isospin chemical potential makes the deconfinement transition stronger. The same property is seen in the  $N_f = 2$  case [24].

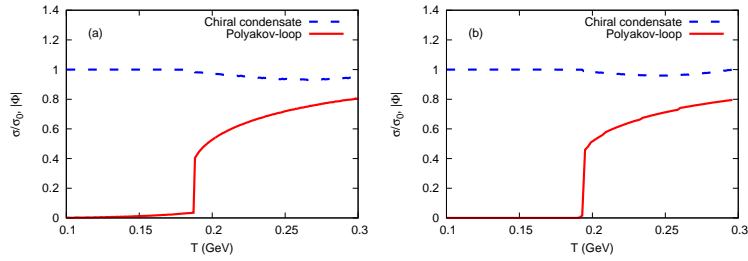


Fig. 3:  $T$  dependence of the chiral condensate  $\sigma$  and the absolute value  $|\Phi|$  at  $\theta = 2\pi/3$ . The PNJL calculation is done with set R in panel (a) and set S in panel (b). The chiral condensate  $\sigma$  is normalized by the value  $\sigma_0$  at  $T = 0$ .

In the RW phase, the isospin symmetry between  $u$  and  $d$  is also broken due to the spontaneous breaking of  $\mathcal{C}$  symmetry [22]. Figure 4(a) shows  $T$  dependence of  $\sigma_f$  at  $\theta = 2\pi/3$  for the case of set R. As a consequence of the isospin symmetry breaking, one of light quarks becomes heavier, while the other becomes lighter.

Figure 3(b) is the same as Fig. 3(a), but the PNJL calculation is done with set S. The order parameters  $\sigma$  and  $\Phi$  have similar  $T$  dependence to those in Fig. 3(a). However,  $\Phi$  is zero below  $T_D = 194$  MeV, since  $\mathbb{Z}_3$  symmetry is exactly preserved.  $\mathbb{Z}_3$  symmetry is spontaneously broken above  $T_D$ . In this case, the confinement/deconfinement phase transition is governed by  $\mathbb{Z}_3$  symmetry. Figure 4(b) is the same as Fig. 4(a), but the PNJL calculation is done with set S. In panel (b), two of three quarks are always degenerate and become heavier at  $T > T_D$ , while one of them becomes lighter there. The flavor symmetry broken by the TBC is found to be recovered in the confinement phase below  $T_D$ .

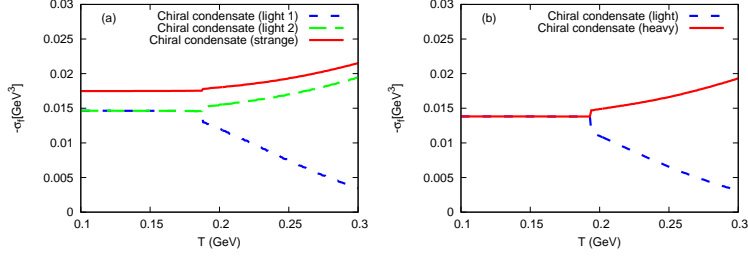


Fig. 4:  $T$  dependence of the chiral condensates  $\sigma_f$  at  $\theta = 2\pi/3$ . The PNJL calculation is done with set R in panel (a) and set S in panel (b). In panel (a), the solid line represents s-quark, while the dashed and dotted lines correspond to light quarks. In panel (b), the solid and dashed lines agree with each other.

### C. Phase diagram in the $\theta$ - $T$ plane

Comparing Fig. 2 with Fig. 3, one can predict that there exists a critical endpoint (CEP) of deconfinement transition in the  $\theta$ - $T$  plane. In fact, the CEP appears at  $\theta = \theta_{\text{CEP}} = 0.62 \times 2\pi/3 = 0.41\pi$ , since the transition changes the order from crossover to first order there. Figure 5 shows  $T$  dependence of  $\chi_{\Phi_R\Phi_R}$ ,  $\chi_{\Phi_I\Phi_I}$  and  $\chi_{\sigma\sigma}$  at  $\theta = \theta_{\text{CEP}}$ . The susceptibility  $\chi_{\Phi_R\Phi_R}$  diverges at  $T = T_{\text{CEP}} = 175$  MeV. This indicates that the deconfinement phase transition is second order just on the CEP. Since  $\Phi_R$  and  $\sigma$  are  $\mathcal{C}$ -even, they can be correlated with each other. In fact,  $\chi_{\sigma\sigma}$  has a divergent peak on the CEP, although it has another peak at higher  $T$ . Meanwhile,  $\Phi_I$  is  $\mathcal{C}$ -odd, so that it is not divergent on the CEP, although it rapidly decreases there.

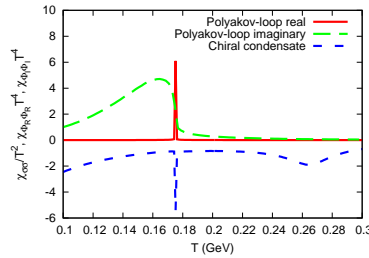


Fig. 5:  $T$  dependence of  $\chi_{\sigma\sigma}$ ,  $\chi_{\Phi_R\Phi_R}$  and  $\chi_{\Phi_I\Phi_I}$  at  $\theta = \theta_{\text{CEP}}$ . The PNJL calculation is done with set R.  $\chi_{\sigma\sigma}$  is multiplied by -1.  $\chi_{\Phi_R\Phi_R}$  is divided by 10, while  $\chi_{\Phi_I\Phi_I}$  is multiplied by 100.

As mentioned in Sec. II,  $\Phi$  becomes zero at some value  $\theta_{\text{conf}}$  of  $\theta$  when  $T$  is small, and  $\theta_{\text{conf}}$  is  $2\pi/3$  for three degenerate flavors and less than  $2\pi/3$  for 2+1 flavors. Figure 6 shows  $\theta$  dependence of  $\Phi$  at low  $T$ . The PNJL calculation is done for three cases of set R, set S and set H. The value

of  $\theta_{\text{conf}}$  is  $2\pi/3$  for set S ( $m_s = 5.5$  MeV),  $\sim 0.85 \times 2\pi/3 = 0.56\pi$  for set R ( $m_s = 140.7$  MeV) and  $\sim 0.75 \times 2\pi/3 = \pi/2$  for set H ( $m_s = 600$  MeV). The set-H case agrees with the two-flavor case [24]. Strictly speaking,  $\theta_{\text{conf}}$  depends on  $T$  for 2+1 flavors, but does not for three degenerate flavors, as shown in (28).

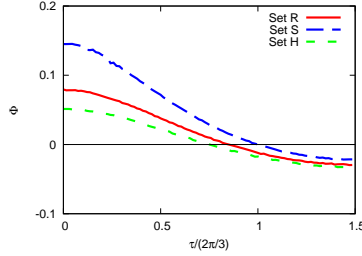


Fig. 6:  $\theta$  dependence of  $\Phi$  at  $T = 150$  MeV. The PNJL calculations are done with three parameter sets of R, S and H.

Figure 7 shows  $T$  dependence of the phase  $\phi$  of  $\Phi$  at  $\theta = 2\pi/3$ . The phase  $\phi$  is  $\mathcal{C}$ -odd and hence an order parameter of  $\mathcal{C}$  symmetry. In panel (a) of set R,  $\phi$  is  $\pi$  at small  $T$ , and it jumps to about  $\pm 2\pi/3$  at high  $T$ . This indicates that  $\Phi$  is negative at small  $T$  and  $\mathcal{C}$  symmetry is broken at high  $T$ . Thus the system is in the RW phase at high  $T$ . Similar result is seen in panel (b) of set S. Here  $\Phi$  is zero at small  $T$  and hence  $\phi$  is not defined there. At high  $T$ ,  $\phi$  is  $\pm 2\pi/3$ .

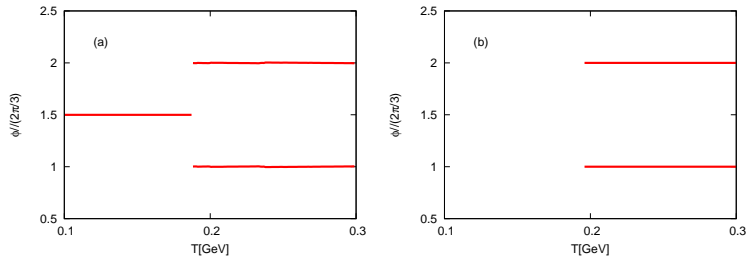


Fig. 7:  $T$ -dependence of the phase  $\phi$  of  $\Phi$  at  $\theta = 2\pi/3$ . The PNJL calculation is done with (a) set R and (b) set S. Note that  $\phi = 4\pi/3 = -2\pi/3 \text{ mod } 2\pi$ .

$T$  dependence of  $\phi$  at  $\theta = 2\pi/3$  shown above is illustrated in Fig. 8 as a movement of  $\Phi$  with respect to increasing  $T$  in the complex  $\Phi$  plane. In panel (a) of set R, the RW phase transition as the spontaneous breaking of  $\mathcal{C}$  symmetry is illustrated by two arrows from some negative value. The transition is mirror-symmetric about the real  $\Phi$  axis in virtue of  $\mathcal{C}$  symmetry. In panel (b) of set S, the deconfinement transition as the spontaneous breaking of  $\mathbb{Z}_3$  symmetry is illustrated by

three arrows. The transition is  $\mathbb{Z}_3$ -symmetric and a jump of  $\Phi = 0$  to  $\Phi = \Phi', \Phi' e^{\pm 2\pi/3}$  for positive  $\Phi'$  smaller than 1.

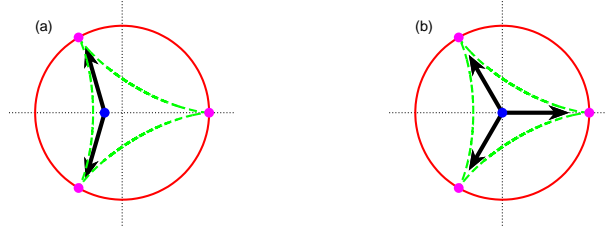


Fig. 8: Typical movement of  $\Phi$  at  $\theta = 2\pi/3$  in (a) set R and (b) set S. The Polyakov loop  $\Phi$  is not allowed to move outside the dashed lines, since the Polyakov-loop potential diverges on the dashed lines.

Figure 9 shows  $\theta$  dependence of  $\phi$  at high  $T$ . The  $\theta$  dependence is symmetric with respect to the line  $\theta = \pi$ , so we consider a range of  $0 \leq \theta \leq \pi$  only. In panel (a) of set R,  $\phi$  is zero at  $0 \leq \theta < 0.91 \times 2\pi/3 = 0.61\pi$ , but diverges into two solutions  $\phi \approx \pm 2\pi/3$  at  $\theta > 0.61\pi$ . The system is in the RW phase when  $\theta > 0.61\pi$ ; here one solution is a  $\mathcal{C}$  image of the other solution. Similar result is seen in panel (b) of set S;  $\phi$  is zero at  $0 \leq \theta < 2\pi/3$ , while  $\phi \approx \pm 2\pi/3$  at  $\theta > 2\pi/3$ .

The RW phase transition was discovered first in the  $\theta_q$ - $T$  plane [6], where  $\theta_q$  is the dimensionless imaginary quark-number chemical potential defined by the quark-number chemical potential  $\mu_q$  as  $\mu_q = iT\theta_q$ . The quark-number density is discontinuous at  $\theta_q = \pi/3 \bmod 2\pi/3$ , when  $T$  is higher than some temperature  $T_{\text{RW}}$ . This first-order phase transition is now called the RW phase transition. It was found in Ref. [22] that  $\mathcal{C}$  symmetry is also spontaneously broken in the RW phase transition. One can then define the RW phase transition by the spontaneous breaking of  $\mathcal{C}$  symmetry. In the  $\theta_q$ - $\theta$ - $T$  space, the RW phase appears as a plane of  $\theta_q = 0$ ,  $\theta_0 \leq \theta \leq \pi$  and  $T > T_{\text{RW}}$ . Here  $\theta_0$  is a critical value of  $\theta$  and depends on  $T$  for set R but not for set S; for example,  $\theta_0 = 0.93 \times 2\pi/3$  at  $T = 250$  MeV for set R and  $2\pi/3$  at  $T > T_{\text{RW}}$  for set S.

Figure 10 shows the phase diagram in the  $\theta$ - $T$  plane. Three panels correspond to parameter sets of R, S and H, respectively. In panel (a) of set R, as mentioned above, there is a CEP of deconfinement transition at  $\theta_{\text{CEP}} = 0.41\pi$  and  $T_{\text{CEP}} = 175$  MeV. Meanwhile, the chiral transition is crossover. Phase diagrams for set S and set H have almost the same structure as that for set R, as shown in panels (b) and (c). The dot-dashed line (the left boundary of RW phase) and the dot-dot-dashed line (the line of  $\Phi = 0$ ) are shifted to the left, when  $m_s$  becomes heavy. The shift of

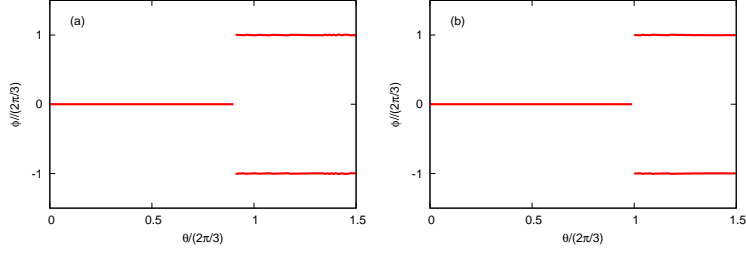


Fig. 9:  $\theta$ -dependence of the phase  $\phi$  of  $\Phi$  at  $T = 250\text{MeV}$ . The PNJL calculation is done with (a) set R and (b) set S.

the dot-dot-dashed line indicates that the confinement at  $\theta = 0$  becomes stronger as  $m_s$  increases. In all the cases, the chiral restoration is weakened at large  $\theta$ , so the chiral-transition lines are not shown there.

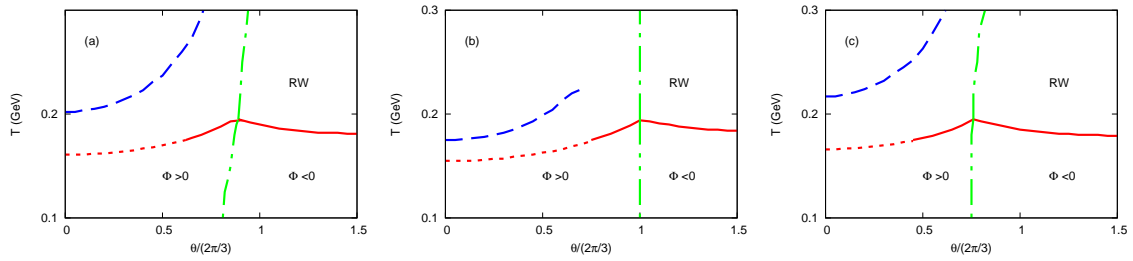


Fig. 10: Phase diagram in the  $\theta$ - $T$  plane. The PNJL calculation is done with (a) set R, (b) set S and (c) set H. The solid, dotted, dashed lines represent first-order deconfinement, crossover deconfinement and crossover chiral transitions, respectively. The dot-dashed line is the left boundary of the RW phase, while the lower boundary of the RW phase is the solid line. The dot-dot-dashed line is the line on which  $\Phi = 0$ . Below the RW region,  $\Phi$  becomes negative.

In Fig. 11,  $|\Phi|$  is plotted as a function of  $\theta$  and  $T$ . For large  $\theta$ ,  $|\Phi|$  has an abrupt jump as  $T$  increases. This jump indicates that the deconfinement transition is first order. As  $\theta$  decreases, the order of the deconfinement transition is changed into crossover. The crossover deconfinement transition at  $\theta = 0$  is thus a remnant of the first-order deconfinement transition at large  $\theta$ .

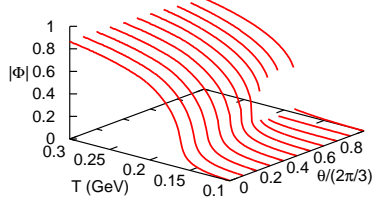


Fig. 11: The absolute value of  $\Phi$  as a function of  $\theta$  and  $T$ . The PNJL calculation is done with set R.

#### D. Susceptibilities at zero and finite $\theta$

Figure 12(a) shows  $T$  dependence of the non-diagonal element  $\chi_{us}$  of quark number density susceptibilities and its derivative  $\chi_{us,T}$  with respect to  $T$  for the case of  $\theta = 0$ . As an interesting property,  $\chi_{us}$  suddenly changes near  $T_D = 161$  MeV, and consequently  $|\chi_{us,T}|$  has a peak there. Comparing  $\chi_{us}$  in Fig. 12(a) with  $\chi_{\Phi_1\Phi_1}$  in Fig. 2(b) shows that that the two quantities are strongly correlated with each other.

The interplay between  $\chi_{us}$  and  $\chi_{\Phi_1\Phi_1}$  can be understood as follows. The stationary condition

$$\frac{\partial}{\partial \varphi_i} \Omega(T, \mu, \varphi) = 0 \quad (30)$$

and its derivatives

$$\frac{D}{D\mu_f} \left[ \frac{\partial}{\partial \varphi_i} \Omega(T, \mu, \varphi(T, \mu)) \right] = 0, \quad (31)$$

lead to a relation between  $\chi_{ff'}$  and  $\chi_{\varphi_i\varphi_j}$  as

$$\begin{aligned} \chi_{ff'} &= -\frac{D^2 \Omega}{D\mu_f D\mu_{f'}} \\ &= -\frac{\partial^2 \Omega(T, \mu, \varphi)}{\partial \mu_f \partial \mu_{f'}} \\ &\quad + \frac{\partial^2 \Omega(T, \mu, \varphi)}{\partial \mu_f \partial \varphi_i} \chi_{\varphi_i \varphi_j} \frac{\partial^2 \Omega(T, \mu, \varphi)}{\partial \mu_{f'} \partial \varphi_j}. \end{aligned} \quad (32)$$

For later convenience, we define  $\partial_X = \partial/\partial X$ . As for  $\chi_{us}$ , the second derivative  $\partial_{\mu_u} \partial_{\mu_s} \Omega$  vanishes at  $\mu_f = 0$ , since  $\Omega$  is  $\mu_f$ -even for each  $f$  and hence  $\partial_{\mu_u} \partial_{\mu_s} \Omega$  is  $\mu_f$ -odd. Similarly,  $\mu_f$ -odd quantities  $\partial_{\mu_f} \partial_{\sigma} \Omega$ ,  $\partial_{\mu_f} \partial_{\sigma'} \Omega$  and  $\partial_{\mu_f} \partial_{\Phi_R} \Omega$  vanish at  $\mu_f = 0$ , whereas a  $\mu_f$ -even quantity  $\partial_{\mu_f} \partial_{\Phi_1} \Omega$  does not. These properties lead to

$$\chi_{us} = \frac{\partial^2 \Omega(T, \mu_u, \varphi)}{\partial \mu_u \partial \Phi_1} \chi_{\Phi_1 \Phi_1} \frac{\partial^2 \Omega(T, \mu_u, \varphi)}{\partial \mu_s \partial \Phi_1} \quad (33)$$



Thus  $\chi_{us}$  is correlated with not  $\chi_{\Phi_R\Phi_R}$  but  $\chi_{\Phi_1\Phi_1}$ . The PNJL result shown in Fig. 12(a) well simulates  $T$  dependence of  $\chi_{us}$  calculated with LQCD [47, 48], although the former underestimates the latter for the magnitude of  $\chi_{us}$ . This underestimation may stem from the fact that the present model does not treat baryon degrees of freedom explicitly.

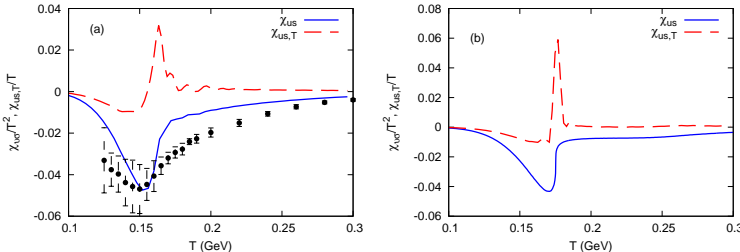


Fig. 12:  $T$  dependence of quark number susceptibility  $\chi_{us}$  (solid line) and its derivative (dashed line) with respect to  $T$  for (a)  $\theta = 0$  and (b)  $\theta = \theta_{\text{CEP}}$ . The PNJL calculation is done with set R, and the resultant  $\chi_{us}$  is multiplied by 20. The corresponding LQCD result [47], shown by dots with errorbars in panel (a), are not normalized.

Similar behavior is seen on the CEP, as shown in Fig. 12(b). The relation (33) persists for finite  $\theta$ , since  $\mathcal{C}$  symmetry is preserved there. Therefore  $|\chi_{us}|$  rapidly decreases at  $T = T_{\text{CEP}}$ , and consequently  $\chi_{us,T}$  has a peak there. The peak is even more conspicuous for  $\theta = \theta_{\text{CEP}}$  than for  $\theta = 0$ .

#### IV. SUMMARY

We have investigated the confinement mechanism in three-flavor QCD with finite imaginary isospin chemical potentials  $(\mu_u, \mu_d, \mu_s) = (i\theta T, -i\theta T, 0)$ , using the PNJL model. Two cases of three degenerate flavors and 2+1 flavors were taken. In the former case, the system has  $\mathbb{Z}_3$  symmetry at  $\theta = 2\pi/3$ . The symmetry is not spontaneously broken for low  $T$  and hence the Polyakov loop  $\Phi$  is zero there. In the latter case,  $\mathbb{Z}_3$  symmetry is explicitly broken for any  $\theta$ , but  $\Phi$  becomes zero at  $\theta = \theta_{\text{conf}}$  smaller than  $2\pi/3$ . Thus the confinement phase defined by  $\Phi = 0$  is realized, even if the system does not have  $\mathbb{Z}_3$  symmetry exactly. In the confinement phase, the static-quark free energy,  $-T \ln[\Phi]$ , diverges. This means that one can consider the confinement by using  $\Phi$  and regard it as an order parameter of the confinement/deconfinement transition, even if  $\mathbb{Z}_3$  symmetry is not preserved exactly.

The phase diagram is determined in the  $\theta$ - $T$  plane. There is a CEP of deconfinement transition at a finite value  $\theta_{\text{CEP}}$  of  $\theta$ . This is a good contrast with the CEP of chiral transition at real quark-number chemical potential. As another interesting point, there is a line of  $\bar{\Phi} = 0$  for both cases of three degenerate flavors and 2+1 flavors. On the line, the confinement phase is realized and the thermodynamic potential has only three-quark configurations in which red, green and blue quarks are statistically in the same state. This property is independent of whether the system has  $\mathbb{Z}_3$  symmetry or not.

In the  $\theta$ - $T$  plane, the confinement transition is crossover on the axis of  $\theta = 0$ , while it is first order on the line of  $\bar{\Phi} = 0$ . This means that the deconfinement crossover at  $\theta = 0$  is a remnant of the first-order deconfinement transition on the line of  $\bar{\Phi} = 0$ . Hence the distance of the line of  $\bar{\Phi} = 0$  from the axis of  $\theta = 0$  shows how strong the confinement property is at  $\theta = 0$ . The line of  $\bar{\Phi} = 0$  is moved to smaller  $\theta$ , as  $m_s$  increases. This means that the confinement property is stronger in the two-flavor case than in the 2+1 flavor case. This statement may be consistent with LQCD results [33, 68, 71]. The non-diagonal element  $\chi_{us}$  of quark number susceptibilities is correlated with not  $\chi_{\bar{\Phi}_R \bar{\Phi}_R}$  but  $\chi_{\bar{\Phi}_I \bar{\Phi}_I}$  for zero and finite  $\theta$ . Hence  $|\chi_{us}|$  does not have a peak near the pseudocritical temperature defined by  $\chi_{\bar{\Phi}_R \bar{\Phi}_R}$ , but rapidly changes there. As a consequence of this property, its derivative  $\chi_{us,T}$  has a peak there. The peak is more conspicuous for finite  $\theta$  than for zero  $\mu$ .

The present results are derived with the PNJL model, but these can be checked by LQCD simulations directly, since the simulations are free from the sign problem for imaginary isospin chemical potential.

### Acknowledgments

The authors thank A. Nakamura, T. Saito, K. Nagata and K. Kashiwa for useful discussions. H.K. also thanks M. Imachi, H. Yoneyama, H. Aoki and M. Tachibana for useful discussions. T.S. is supported by JSPS KAKENHI Grant Number 23-2790. Y.S. is supported by RIKEN Special Postdoctoral Researchers Program.

---

[1] A. M. Polyakov, Phys. Lett. **72B**, 477 (1978).

- [2] H. Kouno, Y. Sakai, T. Makiyama, K. Tokunaga, T. Sasaki, and M. Yahiro, *J. Phys. G: Nucl. Part. Phys.* **39**, 085010 (2012).
- [3] Y. Sakai, H. Kouno, T. Sasaki, and M. Yahiro, arXiv:1204.0228 [hep-ph](2012).
- [4] L. Susskind, *Phys. Rev. D* **20**, 2610 (1979).
- [5] L. D. McLerran, and B. Svetitsky, *Phys. Lett.* **98B**, 195 (1981).
- [6] A. Roberge and N. Weiss, *Nucl. Phys.* **B275**, 734 (1986).
- [7] O. Philipsen, arXiv:1009.4089v1[hep-lat] (2010).
- [8] P. N. Meisinger, and M. C. Ogilvie, *Phys. Lett. B* **379**, 163 (1996).
- [9] A. Dumitru, and R. D. Pisarski, *Phys. Rev. D* **66**, 096003 (2002); A. Dumitru, Y. Hatta, J. Lenaghan, K. Orginos, and R. D. Pisarski, *Phys. Rev. D* **70**, 034511 (2004); A. Dumitru, R. D. Pisarski, and D. Zschiesche, *Phys. Rev. D* **72**, 065008 (2005).
- [10] K. Fukushima, *Phys. Lett. B* **591**, 277 (2004)..
- [11] C. Ratti, M. A. Thaler, and W. Weise, *Phys. Rev. D* **73**, 014019 (2006); C. Ratti, S. Rößner, M. A. Thaler, and W. Weise, *Eur. Phys. J. C* **49**, 213 (2007).
- [12] E. Megias, E. Ruiz Arriola, and L. L. Salcedo, *Phys. Rev. D* **74**, 065005 (2006).
- [13] S. Rößner, C. Ratti, and W. Weise, *Phys. Rev. D* **75**, 034007 (2007).
- [14] B. -J. Schaefer, J. M. Pawłowski, and J. Wambach, *Phys. Rev. D* **76**, 074023 (2007).
- [15] H. Abuki, R. Anglani, R. Gatto, G. Nardulli, and M. Ruggieri, *Phys. Rev. D* **78**, 034034 (2008).
- [16] K. Fukushima, *Phys. Rev. D* **77**, 114028 (2008).
- [17] K. Kashiwa, H. Kouno, M. Matsuzaki, and M. Yahiro, *Phys. Lett. B* **662**, 26 (2008).
- [18] Y. Sakai, K. Kashiwa, H. Kouno, and M. Yahiro, *Phys. Rev. D* **77**, 051901(R) (2008); *Phys. Rev. D* **78**, 036001 (2008); Y. Sakai, K. Kashiwa, H. Kouno, M. Matsuzaki, and M. Yahiro, *Phys. Rev. D* **78**, 076007 (2008); K. Kashiwa, M. Matsuzaki, H. Kouno, Y. Sakai, and M. Yahiro, *Phys. Rev. D* **79**, 076008 (2009); K. Kashiwa, H. Kouno, and M. Yahiro, *Phys. Rev. D* **80**, 117901 (2009).
- [19] L. McLerran K. Redlich and C. Sasaki, *Nucl. Phys. A* **824**, 86 (2009).
- [20] Y. Sakai, K. Kashiwa, H. Kouno, M. Matsuzaki, and M. Yahiro, *Phys. Rev. D* **79**, 096001 (2009);
- [21] K. Kashiwa, M. Yahiro, H. Kouno, M. Matsuzaki, and Y. Sakai, *J. Phys. G: Nucl. Part. Phys.* **36**, 105001 (2009).
- [22] H. Kouno, Y. Sakai, K. Kashiwa, and M. Yahiro, *J. Phys. G: Nucl. Part. Phys.* **36**, 115010 (2009); H. Kouno, Y. Sakai, T. Sasaki, K. Kashiwa, and M. Yahiro, *Phys. Rev. D* **83**, 076009 (2011); H. Kouno, M. Kishikawa, T. Sasaki, Y. Sakai, and M. Yahiro, *Phys. Rev. D* **85**, 016001 (2012).

- [23] T. Hell, S. Rößner, M. Cristoforetti, and W. Weise, Phys. Rev. D **81**, 074034 (2010); T. Hell, K. Kashiwa, and W. Weise, Phys. Rev. D **83**, 114008 (2011).
- [24] Y. Sakai, H. Kouno, and M. Yahiro, J. Phys. G: Nucl. Part. Phys. **37**, 105007 (2010).
- [25] A. Bhattacharyya, P. Deb, S. K Ghosh, and R. Ray, Phys. Rev. D **82**, 014021 (2010).
- [26] T. Matsumoto, K. Kashiwa, H. Kouno, K. Oda, and M. Yahiro, Phys. Lett. B **694**, 367 (2011).
- [27] T. Sasaki, Y. Sakai, H. Kouno, and M. Yahiro, Phys. Rev. D **82**, 116004 (2010); Y. Sakai, T. Sasaki, H. Kouno, and M. Yahiro, Phys. Rev. D **82**, 096007 (2010).
- [28] Y. Sakai, T. Sasaki, H. Kouno, and M. Yahiro, Phys. Rev. D **82**, 076003 (2010).
- [29] R. Gatto, and M. Ruggieri, Phys. Rev. D **83**, 034016 (2011).
- [30] O. Lourenço, M. Dutra, A. Delfino, and M. Malheiro, Phys. Rev. D **84**, 125034 (2011); O. Lourenço, M. Dutra, T. Frederico, A. Delfino, and M. Malheiro, Phys. Rev. D **85**, 097504 (2012).
- [31] K. Kashiwa, T. Hell, and W. Weise, arXiv:1106.5025 [hep-ph](2011).
- [32] K. Morita, V. Skokov, B. Friman, and K. Redlich, arXiv:1107.2273 [hep-ph](2011); arXiv:1108.0735 [hep-ph](2011).
- [33] T. Sasaki, Y. Sakai, H. Kouno, and M. Yahiro, Phys. Rev. D **84**, 091901 (2011).
- [34] Y. Sakai, H. Kouno, T. Sasaki, and M. Yahiro, Phys. Lett. B **705**, 349 (2012); T. Sasaki, J. Takahashi, Y. Sakai, H. Kouno, and M. Yahiro, Phys. Rev. D **85**, 056009 (2012).
- [35] F. Buisseret, and G. Lacroix, Phys. Rev. D **85**, 016009 (2012).
- [36] V. Pagura, D. Gomez Dumm, and N. N. Scoccola, Phys. Lett. B **707**, 367 (2012).
- [37] Y. Sakai, T. Sasaki, H. Kouno, and M. Yahiro, J. Phys. G **39**, 035004 (2012).
- [38] M. Stephanov, K. Rajagopal, and E. Shuryak, Phys. Rev. Lett. **81**, 4816 (1999).
- [39] M. Asakawa, U. Heinz, and B. Müller, Phys. Rev. Lett. **85**, 2072 (2000).
- [40] S. Jeon, and V. Koch, Phys. Rev. Lett. **85**, 2076 (2000).
- [41] Y. Hatta, and T. Ikeda, Phys. Rev. D **67**, 014028 (2003);
- [42] H. Fujii, Phys. Rev. D **67**, 094018 (2003).
- [43] V. Koch, A. Majumder, and J. Randrup, Phys. Rev. Lett. **95**, 182301 (2005).
- [44] M. Asakawa and K. Yazaki, Nucl. Phys. **A504**, 668 (1989).
- [45] A. Barducci, R. Casalbuoni, S. De Curtis, R. Gatto, and G. Pettini, Phys. Lett. B **231**, 463 (1989); A. Barducci, R. Casalbuoni, G. Pettini, and R. Gatto, Phys. Rev. D **49**, 426 (1994);
- [46] M. Asakawa, S. Ejiri, and M. Kitazawa, Phys. Rev. Lett. **103**, 262301 (2009).
- [47] S. Borsanyi, Z. Fodor, S. D. Katz, S. Krieg, C. Ratti, and K. Szabó, JHEP **1201**, 138 (2012).

- [48] A. Bazavov, T. Bhattacharya, C. E. DeTar, H.-T. Ding, S. Gottlieb, R. Gupta, P. Hegde, U. Heller, F. Karsch, E. Laermann, L. Levkova, S. Mukherjee, P. Petreczky, C. Schmidt, R. A. Soltz, W. Soeldner, R. Sugar, P. M. Vranas, arXiv:1203.0784 (2012).
- [49] M. Cristoforetti, T. Hell, B. Klein and W. Weise, arXiv:hep-ph/1002.2336 (2010).
- [50] C. Ratti, R. Bellwied, M. Cristoforetti and M. Barbaro, arXiv:hep-ph/1109.6243 (2011).
- [51] Y. Aoki, G. Endrödi, Z. Fodor, S. D. Katz and K. K. Szabó, Nature **443**, 675 (2006).
- [52] Z. Fodor, and S. D. Katz, Phys. Lett. B **534**, 87 (2002).
- [53] P. de Forcrand and O. Philipsen, Nucl. Phys. **B642**, 290 (2002); P. de Forcrand and O. Philipsen, Nucl. Phys. **B673**, 170 (2003).
- [54] M. D’Elia and M. P. Lombardo, Phys. Rev. D **67**, 014505 (2003); Phys. Rev. D **70**, 074509 (2004); M. D’Elia, F. Di Renzo, and M. P. Lombardo, Phys. Rev. D **76**, 114509 (2007);
- [55] H. S. Chen and X. Q. Luo, Phys. Rev. **D72**, 034504 (2005); arXiv:hep-lat/0702025 (2007).
- [56] L. K. Wu, X. Q. Luo, and H. S. Chen, Phys. Rev. **D76**, 034505 (2007).
- [57] M. D’Elia and F. Sanfilippo, Phys. Rev. D **80**, 014502 (2009).
- [58] P. Cea, L. Cosmai, M. D’Elia, C. Manneschi and A. Papa, Phys. Rev. D **80**, 034501 (2009).
- [59] M. D’Elia and F. Sanfilippo, Phys. Rev. D **80**, 111501 (2009).
- [60] P. de Forcrand and O. Philipsen, arXiv:1004.3144 [hep-lat](2010).
- [61] K. Nagata, A. Nakamura, Y. Nakagawa, S. Motoki, T. Saito and M. Hamada, arXiv:0911.4164 [hep-lat](2009); K. Nagata, and A. Nakamura, arXiv:1104.2142 [hep-ph] (2011).
- [62] T. Takaishi, P. de Forcrand and A. Nakamura, arXiv:1002.0890 [hep-lat](2010).
- [63] M. Kobayashi, and T. Maskawa, Prog. Theor. Phys. **44**, 1422 (1970); M. Kobayashi, H. Kondo, and T. Maskawa, Prog. Theor. Phys. **45**, 1955 (1971).
- [64] G. ’t Hooft, Phys. Rev. Lett. **37**, 8 (1976); Phys. Rev. D **14**, 3432 (1976); **18**, 2199(E) (1978).
- [65] E. Megias, E. Ruiz Arriola, and L. L. Salcedo, Phys. Rev. Lett. **109**, 151601 (2012).
- [66] G. Boyd, J. Engels, F. Karsch, E. Laermann, C. Legeland, M. Lütgemeier, and B. Petersson, Nucl. Phys. **B469**, 419 (1996).
- [67] O. Kaczmarek, F. Karsch, P. Petreczky, and F. Zantow, Phys. Lett. B **543**, 41 (2002).
- [68] S. Borsányi, Z. Fodor, C. Hoelbling, S. D. Katz, S. Krieg, C. Ratti, and K. K. Szabo, arXiv:1005.3508 [hep-lat] (2010).
- [69] W. Söldner, arXiv:1012.4484 [hep-lat] (2010).
- [70] K. Kanaya, arXiv:hep-ph/1012.4235 [hep-ph] (2010); arXiv:hep-ph/1012.4247 [hep-lat] (2010).

[71] A. Bazavov et al., Phys. Rev. D **85**, 054503 (2012).

[72] P. Rehberg, S.P. Klevansky and J. Hüfner, Phys. Rev. C **53**, 410 (1996).